Combined Neural Inactivation of Suppressor of Cytokine Signaling-3 and Protein-Tyrosine Phosphatase-1B Reveals Additive, Synergistic, and Factor-Specific Roles in the Regulation of Body Energy Balance

Nadege Briancon,[1] David E. McNay,[1] Eleftheria Maratos-Flier,[1] and Jeffrey S. Flier[1,2]

OBJECTIVE—The adipokine hormone leptin triggers signals in the brain that ultimately lead to decreased feeding and increased energy expenditure. However, obesity is most often associated with elevated plasma leptin levels and leptin resistance. Suppressor of cytokine signaling (SOCS)-3 and protein-tyrosine phosphatase 1B (PTP-1B) are two endogenous inhibitors of tyrosine kinase signaling pathways and suppress both insulin and leptin signaling via different molecular mechanisms. Brain-specific inactivation of these genes individually in the mouse partially protects against diet-induced obesity (DIO) and insulin resistance. The aim of this study was to investigate possible genetic interactions between these two genes to determine whether combined reduction in these inhibitory activities results in synergistic, epistatic, or additive effects on energy balance control.

RESEARCH DESIGN AND METHODS—We generated mice with combined inactivation of the genes coding for SOCS-3 and PTP-1B in brain cells, examined their sensitivity to hormone action, and analyzed the contribution of each gene to the resulting phenotype.

RESULTS—Surprisingly, the Nestin-Cre mice used to mediate gene inactivation displayed a phenotype. Nonetheless, combined inactivation of SOCS-3 and PTP-1B in brain revealed additive effects on several parameters, including partial resistance to DIO and associated glucose intolerance. In addition, synergistic effects were observed for body length and weight, suggesting possible compensatory mechanisms for the absence of either inhibitor. Moreover, a SOCS-3–specific lean phenotype was revealed on the standard diet.

CONCLUSIONS—These results show that the biological roles of SOCS-3 and PTP-1B do not fully overlap and that targeting both factors might improve therapeutic effects of their inhibition in obesity and type 2 diabetes. *Diabetes* **59:3074–3084, 2010**

The costs of publication of this article were defrayed in part by the payment of page charges. This article must therefore be hereby marked "advertisement" in accordance with 18 U.S.C. Section 1734 solely to indicate this fact.

Obesity is a major risk factor for insulin resistance and type 2 diabetes as well as for cardiovascular diseases. Although identification of the adipokine hormone leptin (1) accelerated progress in understanding mechanisms leading to obesity and associated pathologies, much remains to be discovered. Leptin acts on various brain regions including the hypothalamus, ventral tegmental area, and hindbrain (2–10) and regulates energy homeostasis by triggering decreased food consumption and increased energy expenditure. Unfortunately, circulating leptin levels are elevated in most obese humans, and treatment of these patients with leptin was unsuccessful (11,12). Most obesity is associated with central leptin resistance (13) that may result from defects in leptin transport across the blood-brain barrier (14–17) or inflammatory responses in the mediobasal hypothalamus secondary to overnutrition (18,19). Resistance may also result from dysregulation of the leptin receptor intracellular signaling pathway, which prevents appropriate transduction of the leptin signal.

Suppressor of cytokine signaling (SOCS)-3 and protein-tyrosine phosphatase 1B (PTP-1B) suppress cytokine signaling pathways, including the leptin pathway (20–23). Interestingly, the *Socs-3* gene is a target for signal transducer and activator of transcription (STAT) 3, which is a crucial mediator of leptin signaling (24). SOCS-3 levels are increased after leptin injection and in mice with diet-induced obesity (DIO) (16,25–28). Chronic activation of the leptin pathway generates a negative-feedback regulatory loop that is believed to alter central leptin signaling in DIO. Hypothalamic PTP-1B levels are also modulated by chronic leptin administration, inflammation, and high-fat diet (HFD) feeding (23,29–32).

Genetic inactivation of the *Socs-3* or *Ptpn1* (PTP-1B) genes in mouse brain, like whole-body *Socs-3* haploinsufficiency or *Ptpn1* knockout, leads to enhanced leptin sensitivity and resistance to DIO (33–37). However, possible interactions between the two genes have not been explored. In a system where both genes are inactivated, absence of genetic interaction is expected to be revealed by the addition of the effects generated by the absence of either gene. In contrast, evidence of genetic interaction may be invoked if there is a deviation from such additive effects: this includes synergistic and dominant epistatic effects. In addition, combined inactivation of both genes may reveal new pathways in which both SOCS-3 and PTP-1B play a regulatory role. We therefore decided to investigate possible interactions between *Socs-3* and *Ptpn1* by generating mice with combined gene inactivation

in neural progenitor cells using Nestin-Cre mice. Despite a surprising metabolic phenotype displayed by the Nestin-Cre mice, inactivation of both genes in brain revealed additive effects on most parameters studied. Interestingly, synergistic effects were observed for body length and weight, and some factor-specific phenotypes were also revealed.

RESEARCH DESIGN AND METHODS

Generation of Nestin-Cre;Ptpn1$^{lox/lox}$;Socs-3$^{lox/lox}$ mice. *Socs-3^{lox}* mice were obtained from Dr. Yoshimura and *Ptpn1^{lox}* mice from Drs. Bence, Kahn, and Neel (35,38). Mice were backcrossed more than six times on a C57BL/6 (Jackson Laboratories) background. Nestin-Cre mice were from Jackson Laboratory (strain no. 377). Details of the breeding strategy can be found in the online appendix (available at http://diabetes.diabetesjournals.org/cgi/content/full/db10-1436/DC1). Animal protocols were approved by the institutional animal care and use committee.

HFD studies. Nestin-Cre ($n = 7$), floxed ($n = 15$), *Socs-3* ($n = 9$), *Ptpn1* ($n = 10$), and double-mutant ($n = 13$) mice were fed a diet containing 45% kcal from fat and 35% kcal from carbohydrates (Research Diets no. D12451) starting at 6 weeks of age. Body weight was measured weekly. Fat mass was measured by EchoMRI (Echo Medical Systems) after 13 weeks on the diet. Oxygen consumption, heat production, and locomotor activity were measured using a Comprehensive Lab Animal–Monitoring System (CLAMS; Columbia Instruments) over 48 h, following a 2-day acclimation period. Ambulatory activity was determined by infrared beam breaks along the x- and y-axes. Food intake was manually measured over 2 consecutive days from single-caged animals after a period of habituation. Mice were killed after 21–30 weeks on the diet.

Hormonal assays. Blood was collected from tail nicks in the morning between 0800 h and 1000 h for fed measurements. For studies on the HFD, mice were food deprived for 6 h prior to bleeding in the afternoon. Total plasma insulin-like growth factor (IGF)-1 (Diagnostics Systems Laboratories), leptin, and insulin (CrystalChem) were assayed by enzyme-linked immunosorbent assays.

Glucose and insulin tolerance tests. For glucose tolerance tests, mice were fasted overnight (15–16 h) and intraperitoneally injected with glucose (1 mg/g body wt). For insulin tolerance tests, mice were fasted for 6 h prior to intraperitoneal injections with insulin (0.5 mU/g body wt Humulin R; Eli Lilly).

Leptin sensitivity tests. Standard diet–fed mice were single housed and habituated to handling for 5 days prior to injections. Mice and food were weighed everyday at 0900 h. Measurements for the last 3 days before injections were averaged and used as baseline values. Saline was intraperitoneally administered for 3 days, followed by mouse recombinant leptin (A.F. Parlow, National Hormone and Peptide Program) twice daily for 3 days (0900 h and 1800 h; dose, 0.75 μg/g; total daily dose, 1.5 μg/g).

Immunohistochemistry for phosphorylated STAT3 (pSTAT3) (Tyr 705; Cell Signaling Technology) was performed on free-floating sections. Overnight-fasted mice were intraperitoneally injected with leptin (3 μg/g) or saline (PBS) and transcardially perfused with 10% formalin under deep anesthesia 3 h after injections. DAB (diaminobenzidine) was used for revelation and hematoxylin for counterstaining. Imaging was carried out on an Axio Imager.A1 microscope (Zeiss), processed with Adobe Photoshop software, and analyzed with MacBiophotonics Image J (National Institutes of Health).

Statistical analysis. Genetic interaction was tested by two-way ANOVA when a significant difference was found by a *t* test between double mutants and Nestin-Cre mice. In the absence of interaction, contribution of each gene to the double knockout phenotype is displayed (two-way ANOVA). In the presence of interaction, differences between single mutants and Nestin-Cre mice were tested by one-way ANOVA and displayed. All results are expressed as means ± SE. Tests were performed using GraphPad Prism (Graphpad, San Diego, CA).

RESULTS

Nestin-Cre mice have a metabolic phenotype. Surprisingly, the Nestin-Cre mice in our study had consistently smaller body weight and length than floxed mice on the standard diet (online appendix Fig. S1*A* and S1*B*). In addition, Nestin-Cre mice had higher adiposity and circulating leptin levels than floxed mice (online appendix Fig. S1*C* and S1*D*). Nestin-Cre mice were also less tolerant to glucose challenge while slightly more sensitive to insulin

administration than floxed mice (online appendix Fig. S1*E* and S1*F* and supplementary RESULTS).

On an HFD, Nestin-Cre mice gained less weight than floxed mice over time (online appendix Fig. S2*A*). Body fat content and circulating leptin levels were not significantly different between the two genotypes after 13 weeks on the HFD (Fig. S2*B* and S2*C*). Nestin-Cre mice maintained a greater sensitivity to insulin than floxed mice that became insulin resistant and had lower basal circulating insulin levels (Fig. S2*D* and S2*E*). However, both genotypes became similarly glucose intolerant (Fig. S2*F*). In light of such a considerable metabolic phenotype, we used Nestin-Cre mice as the control line for our studies with *Socs-3/Ptpn1* mice in order to control for the effect of the *Nestin-Cre* transgene.

Combined inactivation of *Socs-3 and Ptpn1* reveals synergistic effects on body size. Brain-specific combined gene inactivation was confirmed in double-mutant mice using real-time quantitative PCR (online appendix Fig. S3). Analysis of growth of mice deficient for either SOCS-3 or PTP-1B or both in brain revealed that double mutants had significantly lower weight than single mutants and Nestin-Cre mice after 7 weeks on the standard diet (Fig. 1*A*). *Socs-3* mutants were lighter than *Ptpn1* mutants and Nestin-Cre mice across several weeks. However, body weight curves of *Ptpn1* mutants and Nestin-Cre mice were similar. Interestingly, *Socs-3* and *Ptpn1* genes interact in a synergistic manner: the effect observed with combined deletions was larger than the sum of the effects of each gene taken independently (Fig. 1*A, note f*). Thus, on a *Socs-3*–null background, central inactivation of *Ptpn1* affects body weight homeostasis.

The substantially lower weight of double-mutant mice was associated with a shorter body length (Fig. 1*B*). As for body weight, both gene deletions contributed synergistically to this phenotype. In line with their smaller size, double mutants had the lowest circulating IGF-1 levels (Fig. 1*C*). The low body weight of the double mutants might be attributed entirely to their short length. However, double mutants had significantly lower BMI (Fig. 1*D*). This suggests that their body composition is substantially altered.

Double mutants have low adiposity on the standard diet because of a lack of brain SOCS-3. Compared with Nestin-Cre mice, fat mass at 19 weeks was similarly reduced in *Socs-3* and double mutants (Fig. 2*A*). Normalization to body weight (Fig. 2*B*) or to body length using fat mass index (fat mass/height squared) (Fig. 2*C*) led to the same observation. A two-way analysis indicates that the low adiposity of double knockout mice is attributed to the absence of brain SOCS-3, whereas the absence of PTP-1B does not contribute to this phenotype. In addition, lean mass was significantly reduced only in double mutants (Fig. 2*A*). This was also true when normalized to body length (not shown). In addition to reduced fat mass, this is likely to contribute to their low BMI.

Various fat depots were dissected from 7- to 8-month-old animals and weighed. Visceral fat pads (retroperitoneal, perirenal, and gonadal), but not subcutaneous pads, were significantly reduced in double mutants compared with Nestin-Cre mice (Fig. 2*D*). At that age, both gene deletions contributed to this phenotype, although absence of SOCS-3 had the main effect. In addition, whereas visceral fat pads were significantly larger than subcutaneous pad in Nestin-Cre and single-mutant mice (Fig. 2*E*), both depots accounted for similar fractions of total dis-
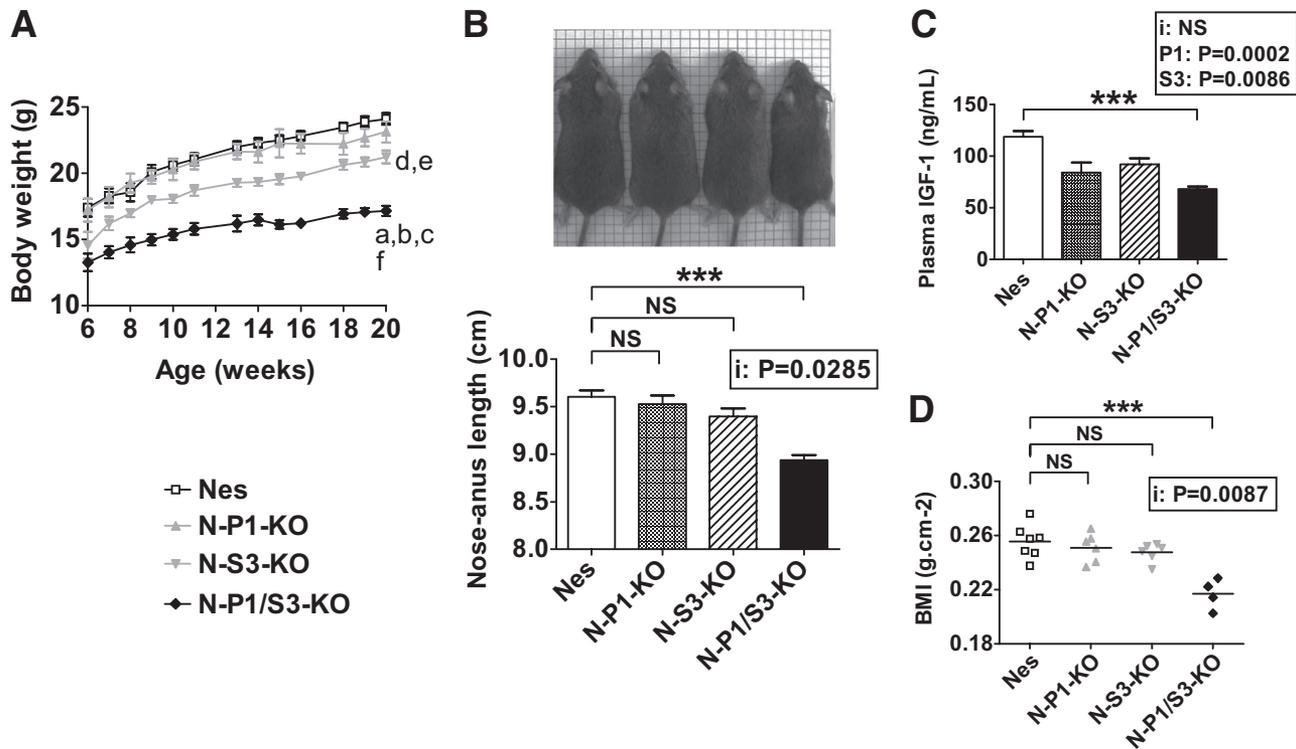
FIG. 1. Double-mutant mice have reduced body length and BMI. *A*: Body weight curve of double mutants (N-P1/S3-KO; *n* = 8), *Ptpn1* (N-P1-KO; *n* = 12), and *Socs-3* (N-S3-KO; *n* = 13) single mutants and Nestin-Cre control mice (Nes; *n* = 6) on the standard diet. One-way ANOVA test followed by Tukey post test gives the following for every time points unless specified: a, *P* < 0.01 vs. Nes; b, *P* < 0.01 vs. N-P1-KO; c, *P* < 0.05 vs. N-S3-KO after week 7; d, *P* < 0.05 vs. Nes (except weeks 6, 8, and 16); e, *P* < 0.05 vs. N-P1-KO between weeks 8 and 15. Interaction between *Socs-3* and *Ptpn1* genes is considered significant (*P* < 0.05) after week 7 by two-way ANOVA (f). *B*: Body length at 5 months (*bottom*) and picture of representative mice for each genotype (*top*). Genetic interaction is statistically significant by two-way ANOVA. *C*: Total plasma IGF-1 levels (*n* = 5–6). Interaction between both genes is not significant. *D*: Double mutants have low BMI. Genetic interaction is significant by two-way ANOVA. Statistical analysis displayed on top of bars and plots was obtained by one-way ANOVA followed by Dunnett test versus Nes. NS, not significant. ***P* < 0.001. Boxed text is result of two-way ANOVA, indicating whether genetic interaction (i) was found. If not, contribution of *Ptpn1* (P1) and *Socs-3* (S3) to the double-mutant phenotype is displayed.

sected pads in double mutants. This suggests that the relative contribution of fat depots to body weight is changed when both *Socs-3* and *Ptpn1* genes are deleted in the brain.

In line with lower adiposity, leptin levels were reduced in double mutants, and this was mainly attributed to the absence of SOCS-3 (Fig. 3*A*). However, neither food intake nor ambulatory activity was different from Nestin-Cre mice (Fig. 3*B* and *C*). A trend toward higher energy expenditure (oxygen consumption and generated heat per kilogram body weight) was observed but did not reach significance (Fig. 3*D* and *E*). Respiratory quotient was unchanged among mutants (Fig. 3*F*).

Double mutants gain less weight on an HFD than Nestin-Cre mice. Both brain *Socs-3*– and *Ptpn1*-null mice were reported to be protected against DIO (34,35). We therefore examined response to DIO in our cohorts. Double mutants weighed significantly less than Nestin-Cre mice until week 14 on the HFD (Fig. 4*A*). Despite the weight effect of the Nestin-Cre transgene, we found that double mutants gained significantly less weight than Nestin-Cre mice over the first 10 weeks on the HFD (*P* < 0.05; comparing Nes and N-P1/S3-KO curves). Both gene deletions contributed to this subtle reduction in weight gain (two-way analysis at week 10: interaction: NS, P1: *P* = 0.01, S3: *P* = 0.01). This protection was nonetheless not total since double mutants still gained substantial weight on the HFD over those on the standard diet (Fig. 4*B*).

Fat mass was measured after 13 weeks on the HFD (Fig.

4*C*). Double mutants had significantly lower adiposity than Nestin-Cre mice, and deletion of *Ptpn1* accounted for this phenotype (two-way ANOVA). However, after 5–7 months on the HFD, no significant difference in fat pad weights was detected between genotypes (Fig. 4*D*). This may reflect a ceiling effect. Nonetheless, visceral fat pads were smaller than subcutaneous depots in double mutants, whereas the opposite was observed for Nestin-Cre and *Ptpn1* mutants (Fig. 4*E*), in line with our observations on the standard diet.

Double mutants have high energy expenditure on the HFD. After 11–13 weeks on the HFD, double mutants had low circulating leptin levels compared with Nestin-Cre mice. This phenotype was attributed to both *Ptpn1* and *Socs-3* deletions (Fig. 5*A*). Although food intake and ambulatory activity were not changed (Fig. 5*B* and *C*), oxygen consumption and heat generated were significantly increased in double-mutant mice (Fig. 5*D* and *E*). In both cases, deletion of *Socs-3* accounted for most of the variance (two-way ANOVA). Respiratory quotient was not changed (Fig. 5*F*). All together, our data indicate that double-mutant mice are more resistant to DIO than Nestin-Cre mice and that this resistance may be attributed to increased energy expenditure.

Leptin sensitivity is enhanced in mice lacking brain SOCS-3 and PTP-1B. The finding of normal food intake and normal to high energy expenditure of double-mutant mice in the context of low circulating leptin levels suggest
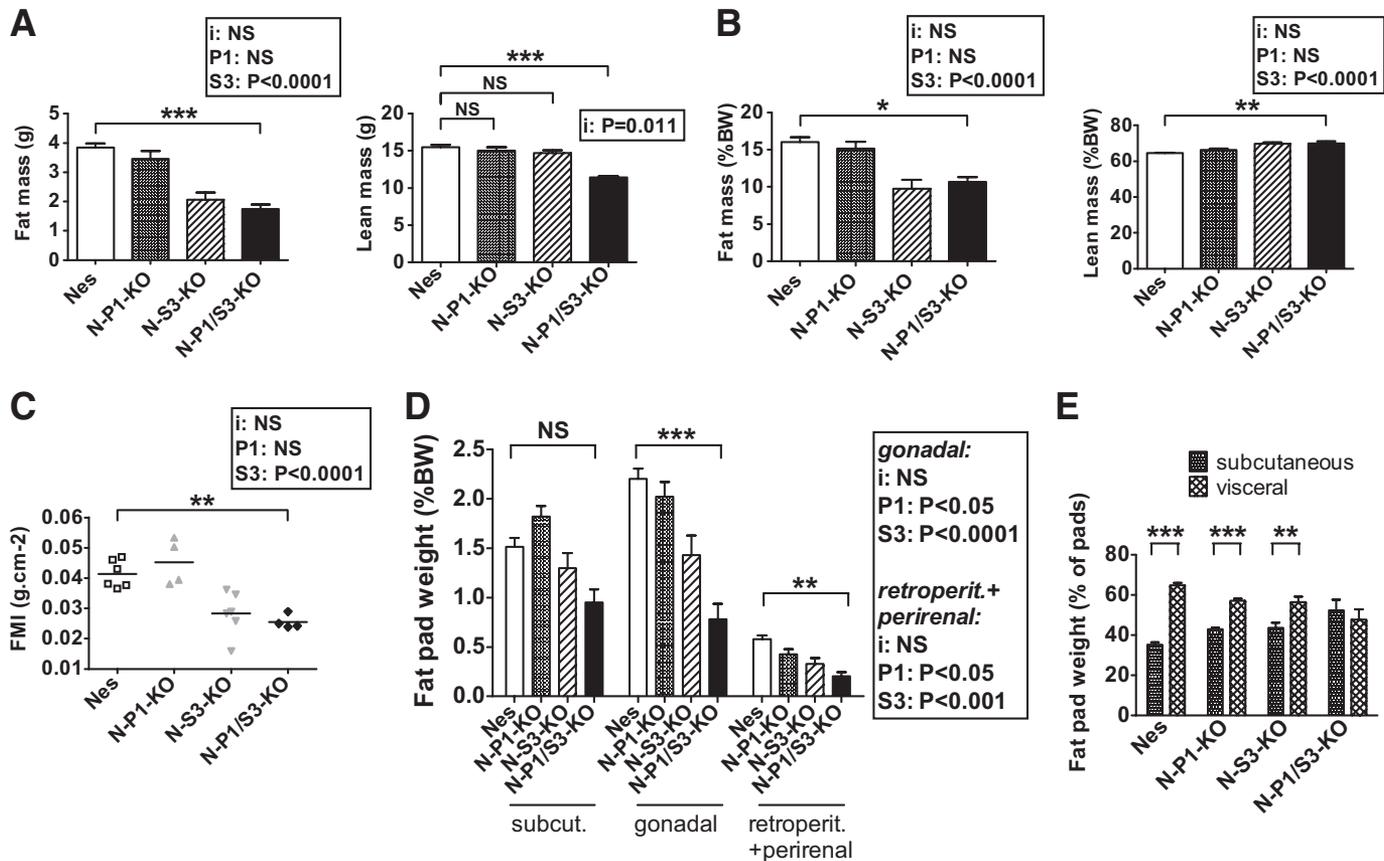
FIG. 2. Double mutants have as low adiposity on the standard diet as *Socs-3* mutants. *A* and *B*: Fat and lean mass was measured by EchoMRI at 19 weeks (*A*) and given in *B* as percentage of body weight (*n* = 6–13). *C*: Fat mass index (FMI). *D* and *E*: Fat pads were carefully dissected when the mice were killed (7–8 months old) and then were weighed, and results are given as percentage of body weight (*D*). Gonadal, retroperitoneal, and perirenal pads are pooled in *E* (= visceral). The contribution of subcutaneous and visceral fat pads to total weight of the dissected pads is displayed (*n* = 5–11). *$P < 0.05$; **$P < 0.01$; ***$P < 0.001$ by one-way ANOVA followed by Dunnett test versus Nes or *t* test. Boxed text, two-way ANOVA (see legend of Fig. 1 for details).

that leptin signaling is enhanced in these mice. Therefore, we examined sensitivity to recombinant leptin.

Upon repeated daily injections of recombinant leptin, 27- to 31-week-old single and double knockout mice demonstrated a greater body weight loss than Nestin-Cre mice on the second day of treatment (Fig. 6*A*, day 5). After 3 days of injections, only double mutants presented a significant body weight loss compared with Nestin-Cre mice. Two-way ANOVA tests indicate that combined gene deletions had similar additive effects. However, in contrast to body weight, we were unable to detect a significant difference between mutant and Nestin-Cre mice in leptin-induced anorexia (Fig. 6*B*).

STAT3 plays a role in propagating the leptin signal and is phosphorylated upon leptin binding to its receptor. Under basal conditions, there were more cells in hypothalamic arcuate nucleus (ARN) with high levels of pSTAT3 in double mutants (Fig. 6*C*), an effect accounted for by *Ptpn1* deletion (two-way ANOVA). Upon leptin injections, only *Socs-3* and double mutants presented a significant increase in the number of ARN cells with high levels of pSTAT3.

The ventromedial nucleus of the hypothalamus (VMN) is another important leptin-responsive brain region involved in body weight and glucose homeostasis (4,39). As in the ARN upon leptin action, the number of leptin responsive pSTAT3+ cells in the VMN was higher in *Socs-3* and double mutants, and absence of *Socs-3* accounted for the phenotype displayed by double mutants.

Despite differences in STAT3 activation, no significant differences were detected in transcript levels of anorexigenic *Pomc1* and orexigenic *Agrp* and *Npy* genes in the ARN between the genotypes, either basally or upon leptin administration in 7- to 11-month-old mice (not shown). This is in accordance with the absence of significant differences in daily food intake in our cohorts.

Glucose homeostasis is improved by combined brain deletions of SOCS-3 and PTP-1B. Because increased adiposity and leptin resistance are associated with insulin resistance leading to diabetes, we evaluated glucose homeostasis in our double mutants, both on the standard diet and HFD.

Glycemia was not different between genotypes on chow diet (Fig. 7*A*). However, double mutants had significantly lower blood glucose levels after 11–13 weeks on the HFD than Nestin-Cre mice. *Socs-3* and *Ptpn1* deletions had similar additive effects on lowering glucose levels (Fig. 7*B*). In addition, circulating insulin levels were lower in double mutants on standard diet and a trend toward low insulin levels on the HFD was observed (Fig. 7*C* and *D*). Interestingly, brain specific *Socs-3* deletion accounted for the low insulinemia displayed by double mutants (Fig. 7*C*, two-way ANOVA). All together, these observations suggest that double mutants are more insulin sensitive than controls on both diets.

Glucose tolerance tests revealed that on both diets, area under the curve was significantly smaller for double mutants compared with Nestin-Cre mice (Fig. 7*E* and *F*).
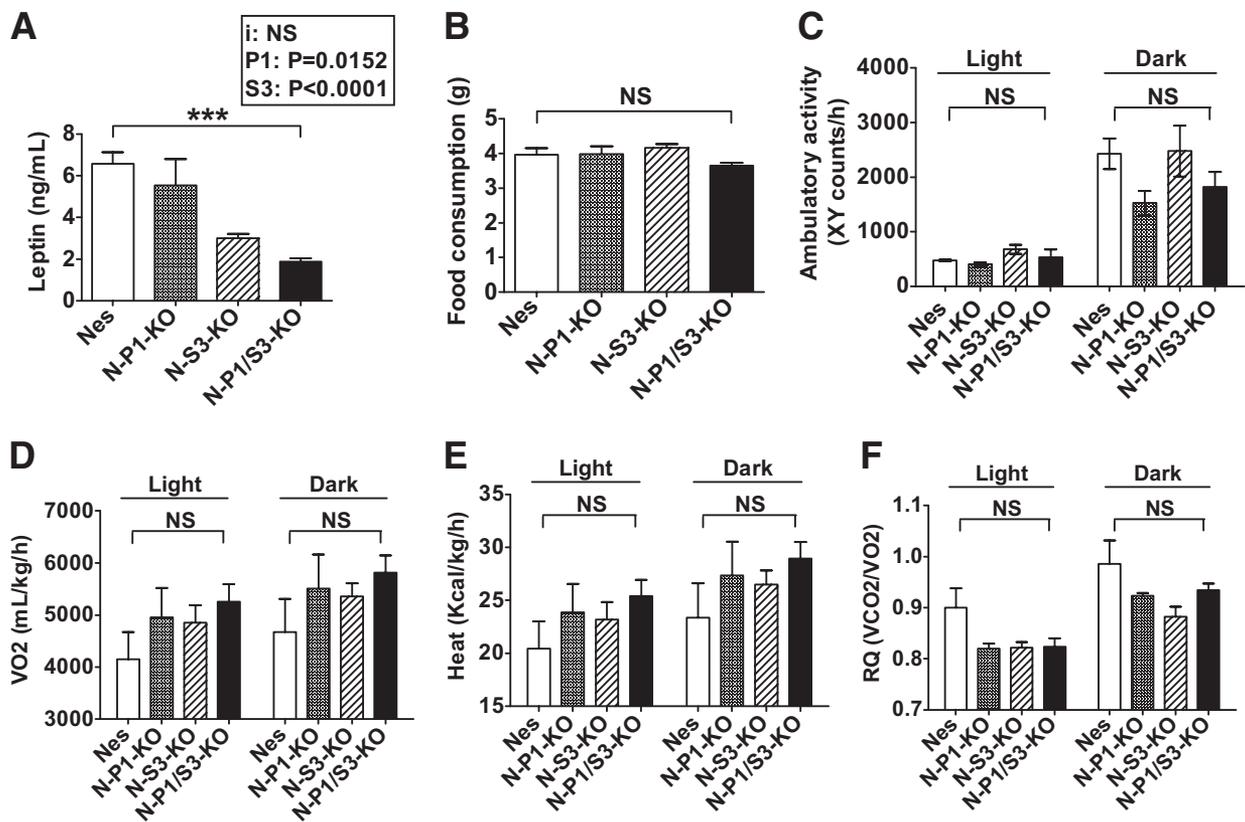
FIG. 3. Energy expenditure is slightly but not significantly increased by combined gene deletions. *A*: Circulating leptin levels of 5-month-old animals (*n* = 4–6). Logarithmic transformation of data were applied for statistical analysis attributed to variance heterogeneity. *B*: Daily standard diet consumption of singly housed 27- to 31-week-old mice (*n* = 5–12). *C* and *F*: Ambulatory activity (*C*), oxygen consumption (*D*), heat generated (*E*), and respiratory quotient (*F*) were recorded over 48 h and shown as average per hour during light and dark cycles (*n* = 4–6). Oxygen consumption and heat are normalized for body weight to account for the animal size differences. NS, not significant. ***$P < 0.001$ by *t* test. Boxed text, two-way ANOVA (see legend of Fig. 1 for details).

On the standard diet, the effect of *Ptpn1* deletion did not quite reach significance and *Socs-3* deletion had the main effect. On HFD, overnight-fasted glucose levels were lower for *Ptpn1* ($P < 0.01$) and double mutants ($P < 0.001$) before injections (Fig. 7*F*). Both gene deletions had additive effects on improving glucose tolerance, although *Socs-3* contributed the most.

Sensitivity to insulin injections was improved for double mutants on both diets as well. On the standard diet, both genes contributed equally to this effect (Fig. 7*G*). On the HFD, double-mutant mice had significantly lower basal glucose levels than Nestin-Cre mice ($P < 0.001$). Deletion of *Socs-3* gene did not quite significantly affect insulin tolerance, while *Ptpn1* deletion had a main effect (two-way ANOVA) (Fig. 7*H*). Hence, insulin sensitivity of double mutants on HFD is improved to an extent comparable to brain *Ptpn1* mutants, while on the standard diet it reflects the similar additive protective effects of each deletion.

DISCUSSION

Although obesity is typically associated with high circulating leptin levels, most obese animals and humans maintain elevated energy intake. Furthermore, in obese rodents, resistance to exogenous leptin led to the concept of leptin resistance (13). Thus, approaches that increase leptin sensitivity may provide insights into developing novel therapies for obesity and associated diseases. SOCS-3 and PTP-1B act as endogenous inhibitors of cytokine signaling

pathways. Importantly, both factors suppress leptin as well as insulin signaling, which makes them potential targets for type 2 diabetes treatment. Indeed, PTP-1B inhibitors are under development or testing in antidiabetic clinical trials (40,41).

To evaluate the possibility that *Socs-3* and *Ptpn1* genes might interact in the regulation of body weight and glucose homeostasis, mice with combined gene deletions in the brain were generated. In the course of these experiments, the Nestin-cre mice, used to mediate gene inactivation, appeared to have an intrinsic metabolic phenotype including reduced body weight and length in the context of increased adiposity on the standard diet but less weight gain on the HFD than floxed controls. These intrinsic phenotypes may mask some of the phenotypes previously reported by brain-specific single-gene mutants. For example, both brain single mutants were reported to be resistant to DIO compared with floxed siblings (34,35). However, in our hands, single mutants were not better protected against DIO than Nestin-Cre mice (one-way analysis), whereas single mutants were when compared with floxed siblings (not shown). Hence, phenotypes caused by presence of the Nestin-Cre transgene are likely to mask subtle phenotypes caused by absence of either SOCS-3 or PTP-1B in our Nestin-Cre–mediated knockout mice.

Phenotypic discrepancies were observed for single mutants between the pioneer studies with the brain *Ptpn1* or *Socs-3* knockout (34,35) and ours. Those discrepancies
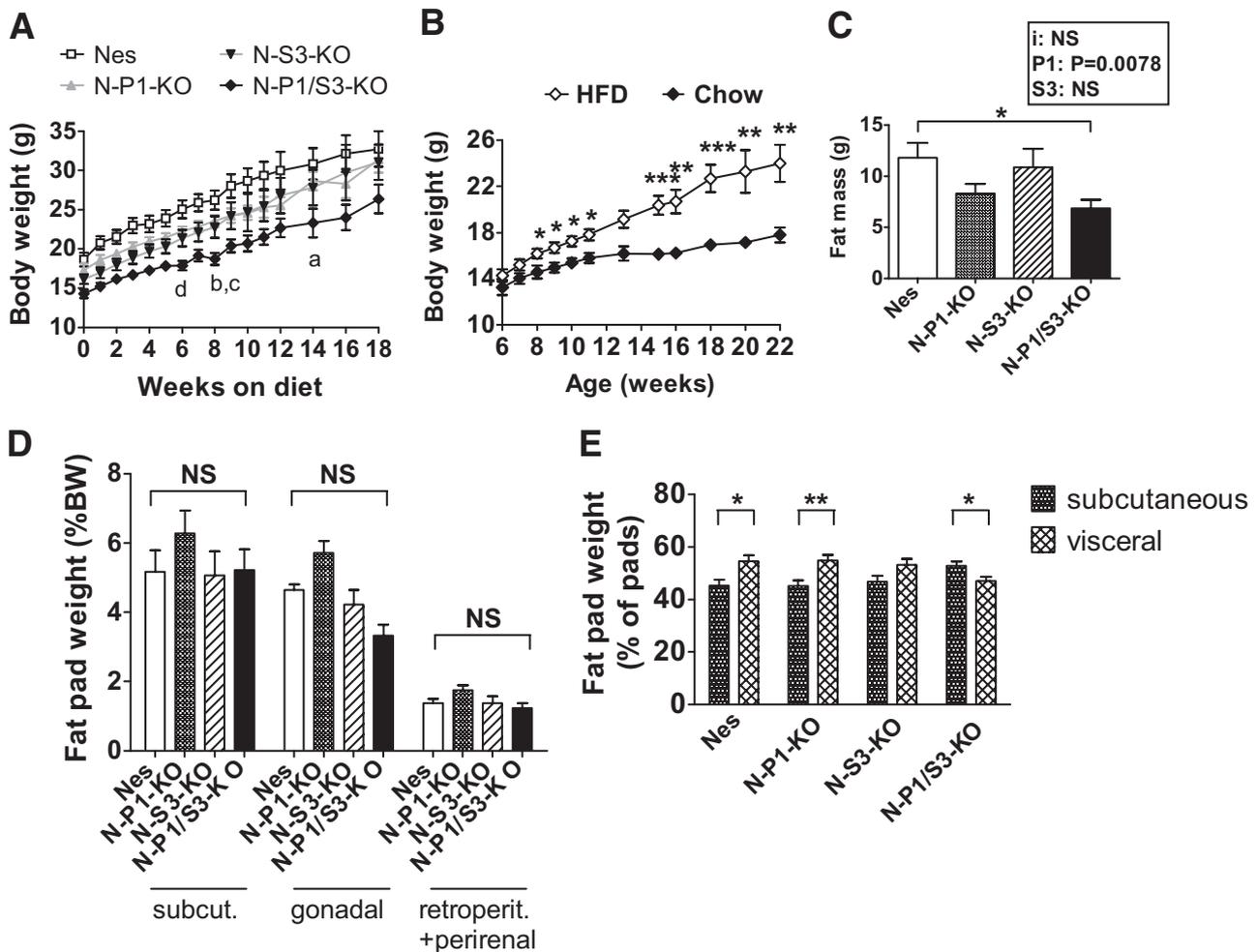
FIG. 4. Double mutants gain less weight on the HDF than Nestin-Cre mice. *A*: Body weight curve on the HFD starting at 6 weeks of age. Statistical analysis is one-way ANOVA followed by Tukey post test. a, $P < 0.05$ for double knockout vs. Nes until week 14. b, $P < 0.05$ for double knockout vs. N-P1-KO until week 8. c, $P < 0.05$ for double knockout versus N-S3-KO for weeks 6 and 8 only. d, $P < 0.05$ for N-S3-KO vs. Nes until week 6. Interaction between *Ptpn1* and *Socs-3* genes is not significant by two-way ANOVA. *B*: Effect of HFD versus standard diet on body weight of double mutants (*$P < 0.05$; **$P < 0.01$; and ***$P < 0.001$ by Welch corrected *t* test). *C*: Fat mass was measured after 13 weeks on the HFD by EchoMRI. *D* and *E*: Fat pad weights given as percentage of body weight (*D*) or of total dissected pads (*E*). NS, not significant. *$P < 0.05$; **$P < 0.01$ (*t* test). Boxed text, two-way ANOVA.

may result from use of different strains of Cre-expressing mice (see above), from diet compositions (different in all three studies), and from genetic background differences. Indeed, marked differences in feeding, energy expenditure, and response to DIO have been reported between C57BL/6 and 129 genetic backgrounds (42).

The finding of a phenotype of Nestin-Cre mice suggests that these mice must be used with caution in metabolic studies. Although our data does not address whether the above described phenotypes are attributed to disruption of gene sequences at the locus of the transgene insertion or to potential Cre toxicity in particular cell types, it has previously been shown that high Cre activity levels are toxic to neural stem/progenitor cells (43).

Despite the metabolic phenotype of Nestin-Cre mice, combined inactivation in brain of *Ptpn1* and *Socs-3* revealed synergistic interactions and additive effects, which ranged from the addition of similar effects to primary and gene-specific effects. No antagonistic functions, some of which may lead to negation of an effect, were revealed. Importantly, the current study was the first direct comparison of the roles of SOCS-3 and PTP-1B in siblings or closely related single knockout mice. The contribution of

each gene to the phenotypes observed in double mutants is summarized in Table 1.

Body length and body weight were the only parameters that revealed synergism between SOCS-3 and PTP-1B actions. Combined brain deletions led to a short body length phenotype. We examined aspects of the growth hormone axis: double mutants had the lowest IGF-1 levels and trended to the lowest growth hormone levels (not shown). This suggests that the growth hormone/IGF-1 axis is centrally affected by loss of SOCS-3 and PTP-1B. Both SOCS-3 and PTP-1B bind to and suppress signaling through the growth hormone and IGF-1 receptors (44–47). Both growth hormone and IGF-1 exert a feedback onto hypothalamic neurons that leads to suppression of growth hormone pituitary secretion. Double mutants might have increased hypothalamic sensitivity to circulating growth hormone and IGF-1, leading to a reduction in growth hormone which in turn leads to reduced IGF-1 secretion and small body size.

This synergism suggests that when only one factor is deleted, compensatory mechanisms substitute to maintain linear growth, and these mechanisms cannot be sustained when both proteins are absent. As we did not observe any
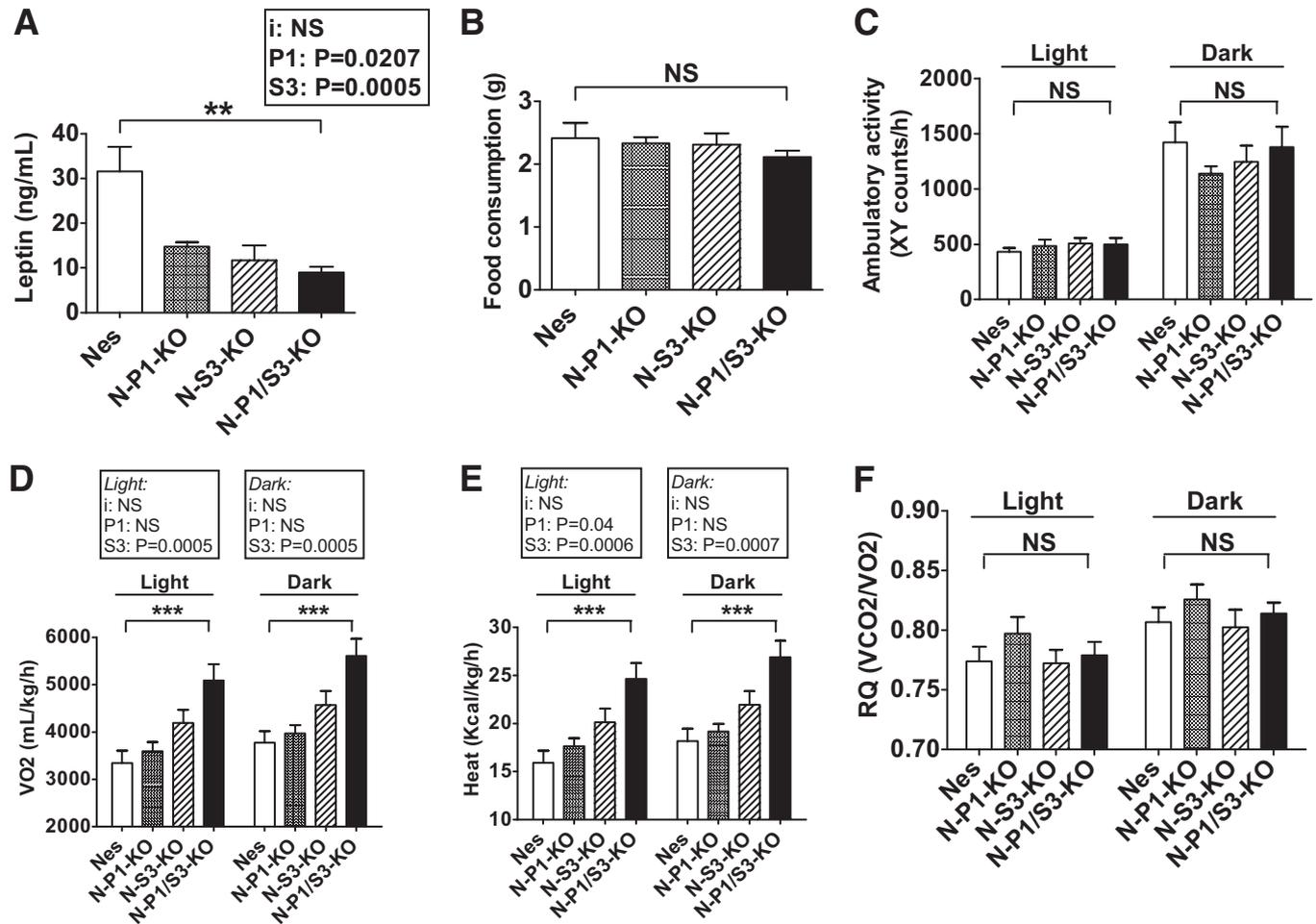
FIG. 5. Double mutants have high energy expenditure on the HFD. *A*: Circulating leptin levels after 11–13 weeks on the HFD ($n = 6$–7). *B*: Daily food consumption after 5–7 months on the HFD. *C–F*: Ambulatory activity (*C*), oxygen consumption (*D*), heat generated (*E*), and respiratory quotient (*F*) on the HFD ($n = 7$–9). NS, not significant. **$P < 0.01$; ***$P < 0.001$ by *t* test. Boxed text, two-way ANOVA.

change in PTP-1B or SOCS-3 expression in *Socs-3* and *Ptpn1* mutants, respectively, compared with Nestin-Cre mice (Fig. S3), possible compensatory mechanisms do not involve upregulation of expression of the other inhibitor in single mutants.

In addition, both SOCS-3 and PTP-1B suppress signaling through receptor-associated Janus kinase 2 (JAK2) and tyrosine kinase receptors, although they have different modes of action: SOCS-3 can interact with and block JAK2 activity, promote degradation of insulin receptor substrate proteins and receptor complex via its SOCS box, and block access to specific cytokine receptor tyrosine residues, whereas PTP-1B is an endoplasmic reticulum–associated enzyme that dephosphorylates and inactivates these same partners, probably following endocytosis of the ligand receptor complex (21–24). We might speculate that in absence of SOCS-3, fewer cytokine receptor complexes may be targeted for degradation by the proteasome, thereby increasing the pool of recycled receptors and leading to increased signal transduction. In the absence of PTP-1B, internalized receptor complexes might remain phosphorylated and hence active for a longer period of time. Combined absence of SOCS-3 and PTP-1B might then result in multiplicative effects of absence of each factor on stability and activity of the same target molecule. However, one might then wonder why this synergistic effect is only detected for body length and not for adiposity

or other parameters. Further investigation is needed to understand the molecular basis of this synergy.

Most phenotypes displayed by the double knockout mice resulted from the addition of the phenotypes displayed by the single knockout mice. For example, inactivation of both genes contributed to the partial protection against DIO and associated hyperglycemia and glucose intolerance displayed by double mutants. Protection against DIO was associated with higher energy expenditure, suggesting that the sympathetic tone may be stimulated in absence of both factors.

Additive effects may underlie independent functions, indicating that the biological roles of SOCS-3 and PTP-1B do not fully overlap. These factors may act on different downstream pathways that contribute to the same phenotypes or on the same pathways but on different targets. However, we cannot rule out that some dominant epistatic effects might not have been revealed because of the difficulty in obtaining large cohorts of single- and double-conditional knockout mice. Interestingly, some phenotypes displayed by the double mutants are largely attributed to the absence in the brain of either SOCS-3 or PTP-1B. For instance, *Ptpn1* deletion transiently has a main effect on adiposity levels on HFD.

In contrast, deletion solely of *Socs-3* is responsible for low adiposity and low insulin levels on the standard diet. Although mice with single deletions had same levels of
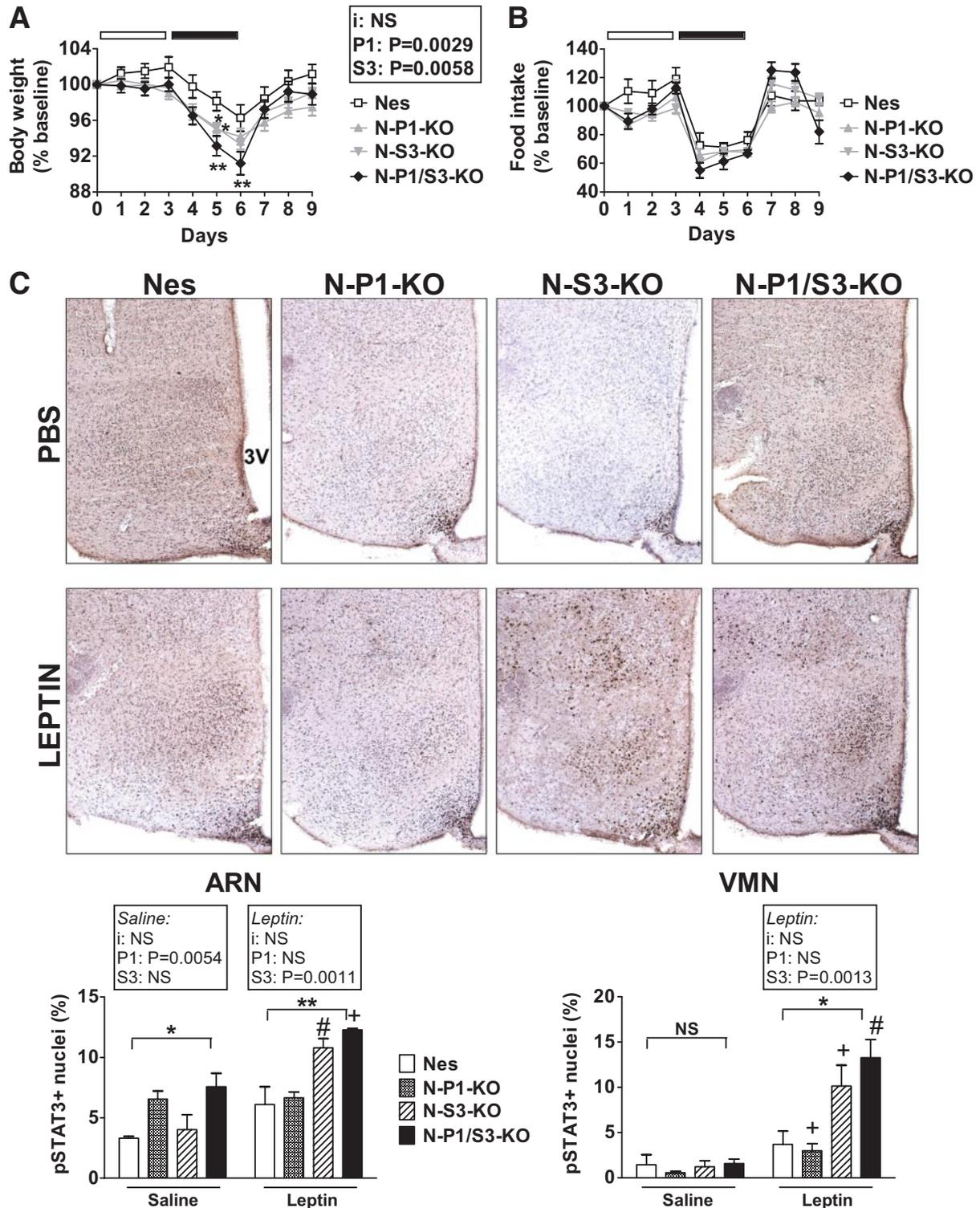
FIG. 6. Double mutants have enhanced leptin sensitivity. *A* and *B*: Leptin sensitivity test. Single-housed 27- to 31-week-old mice were injected daily with saline for 3 days (□) followed by recombinant leptin (■). Body weight (*A*) and food intake (*B*) were monitored on a daily basis (*n* = 5–12). **P* < 0.05 and ***P* < 0.01 by one-way ANOVA with Dunnett test vs. Nes. Interaction between the two genes is not significant by two-way ANOVA. Boxed text, two-way ANOVA. *C*: pSTAT3 was revealed by immunohistochemistry (brown nuclear staining) 3 h after leptin or saline acute injections (*n* = 3 per group). Nucleus counterstaining is Mayer hematoxylin. 3V, third ventricle. Original magnification, ×100. Highly stained hypothalamic pSTAT3+ nuclei were counted from at least three sections per animal through the ARN and VMN nuclei (-1.34 to -2.06 mm relative to Bregma) using Image J and are given as percent of hematoxylin-stained nuclei (histograms). NS, not significant. **P* < 0.05; ***P* < 0.01 by *t* test. Boxed text, two-way ANOVA. + and #: *P* < 0.05 and *P* < 0.01 by *t* test compared with saline injected. (A high-quality digital representation of this figure is available in the online issue.)

food consumption and energy expenditure, *Socs-3* mutants were leaner than *Ptpn1* mutants with lower circulating leptin levels. This suggests that leptin sensitivity is

enhanced in *Socs-3* mutants. However, both single mutants lost similar amount of weight upon repeated leptin administration, indicating comparable leptin sensitivity.
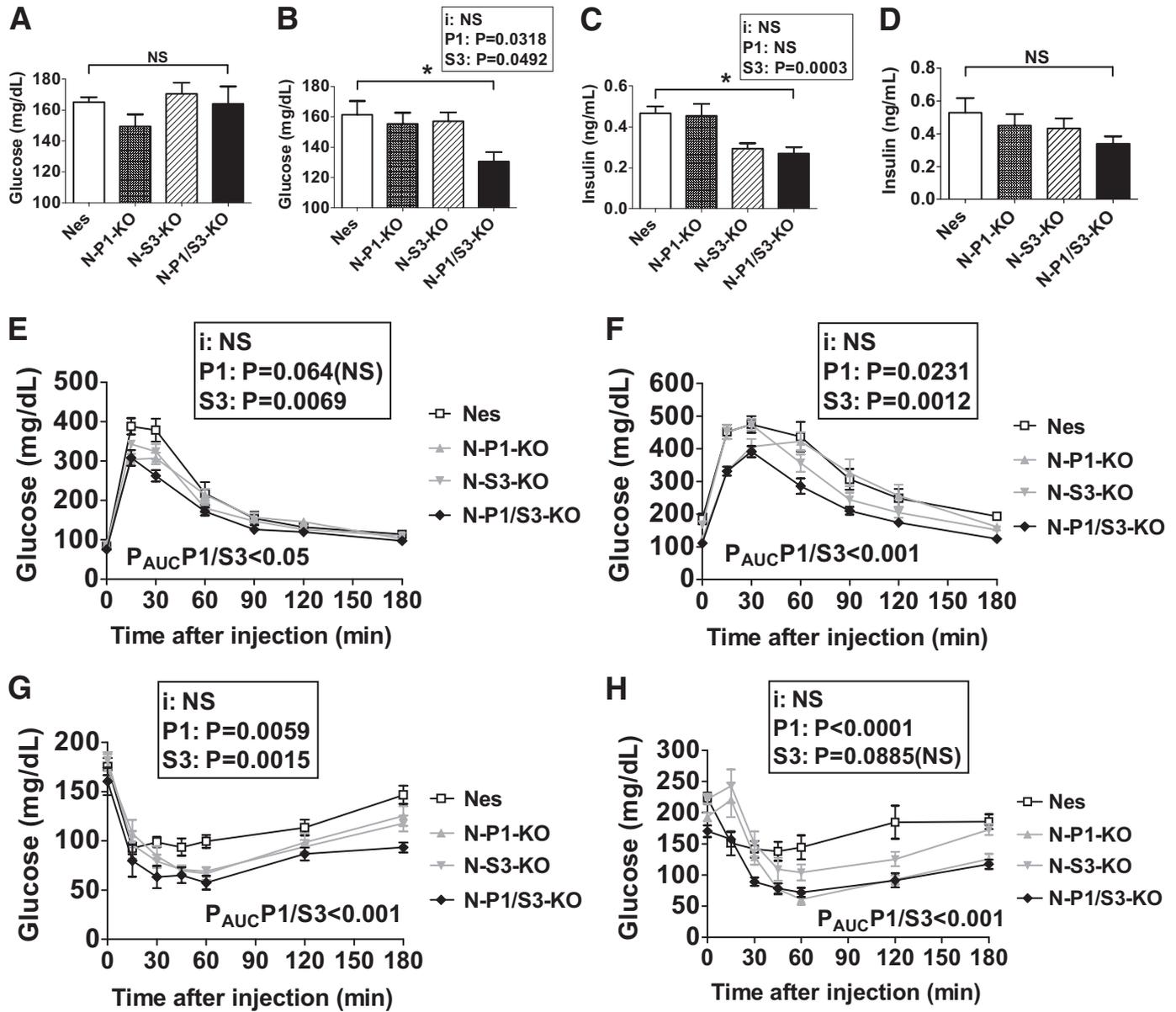
FIG. 7. Glucose homeostasis is enhanced by combined brain deletions of *Socs-3* and *Ptpn1* genes. *A*: Ad libitum blood glucose on the standard diet (*n* = 6–12). *B*: Six-hour fast blood glucose levels after 11–13 weeks on the HFD (*n* = 7–12). *C*: Ad libitum plasma insulin levels on the standard diet (*n* = 5–11). *D*: Six-hour fast plasma insulin levels after 11–13 weeks on the HFD (*n* = 6–8). *E*: Glucose tolerance test after 20–22 weeks on the standard diet (*n* = 5–13). *F*: Glucose tolerance test after 19 weeks on the HFD (*n* = 7–12). *G*: Insulin sensitivity test after 21–23 weeks on the standard diet (*n* = 6–11). *H*: Insulin sensitivity test after 20 weeks on the HFD (*n* = 7–12). NS, not significant. *$P < 0.05$ by *t* test. Same test was performed, with AUC and *P* value for double mutants are displayed (*E–H*). Interaction between the genes is considered not significant for all panels. Boxed text, two-way ANOVA.

Two hypotheses involving either a decrease in energy input or an increase in energy output, might account for such discrepancies.

First, the low power of our CLAMS study may prevent a thorough assessment of energy expenditure. Alternatively, the underlying difference may be beyond the limit of detection of currently available equipment. In fact, upon HFD feeding that challenges metabolic regulatory mechanisms, *Socs-3* deletion accounts for most of the double knockout increase in energy expenditure, suggesting enhanced energy expenditure in *Socs-3* mutants. In addition, a difference in body weight between single mutants is already detectable at 8 weeks on the standard diet and increases at a slow rate afterward. As energy expenditure was assessed at 6–7 months, the older age may prevent the

detection of a small change in energy expenditure. Increased energy expenditure may result from increased sympathetic activity. Low insulin levels of *Socs-3* mutants might then be a consequence of high sympathetic activity, which was shown to affect the bioactivity of a bone-derived insulin segretagogue (48). In turn, low insulin levels might contribute to reduced adipose mass.

Second, our study does not address possible differences in intestinal absorption. Possibly, absence of SOCS-3 affects sympathetic and/or vagal innervations of the digestive tract. Further investigation is required to test these two hypotheses.

Socs-3 mutants had a larger number of pSTAT3+ hypothalamic cells than *Pptn1* mice revealed by immunohistochemistry upon leptin administration, despite having

TABLE 1
Contributions of PTP-1B and SOCS-3 to the phenotypes displayed by double mutants

Diet	PTP-1B	SOCS-3	Interaction
Standard diet			
Phenotype			
Body weight	+	+	S
Body length	+	+	S
Body fat mass	−	+	G
Leptin	+	+*	A
Leptin-induced body weight loss	+	+	A
Leptin-induced pSTAT3 + hypothalamic nuclei	−	+	G
Insulin	−	+	G
Glucose tolerance	+§	+*	A
Insulin sensitivity	+	+	A
HFD			
Phenotype			
Body weight	+	+	A
Body fat mass (13 weeks)	+	−	G
Leptin	+	+	A
Energy expenditure	+	+*	A
Glucose	+	+	A
Glucose tolerance	+	+*	A
Insulin sensitivity	+	−	G

Contribution of each gene deletion to the double knockout phenotype is given by two-way ANOVA (+, contribution to the total variance; −, unlikely contribution). *Main effect. §P value for PTP-1B contribution to this phenotype was close to the cut off value (Fig. 7) and we therefore decided to include its contribution in this chart. A, additive effects; G, gene-specific effects (a subset of additive effects); S, synergistic interaction.

similar leptin sensitivity assessed by leptin-induced body weight loss. This contradiction is only apparent because the immunochemical assay only reveals a subset of leptin sensitive cells (those with large amounts of pSTAT3), whereas not all cells may respond equally well to leptin. The number of poorly versus highly leptin responsive cells might differ between genotypes. Moreover, absence of PTP-1B resulted in an increased number of ARN pSTAT3+ cells under basal conditions, suggesting enhanced basal leptin sensitivity in *Ptpn1* and double mutant arcuate nuclei.

Surprisingly, fat depots are not equally affected by combined loss of SOCS-3 and PTP-1B in brain. Indeed, double mutants presented a reduction in visceral fat pads, whereas subcutaneous pads were less affected. Subcutaneous fat is believed to have beneficial effects on glucose tolerance and insulin sensitivity as opposed to visceral fat (49). Therefore, this phenotype in turn may contribute to the enhanced insulin and glucose sensitivity observed in double mutants.

In our study, inactivation of SOCS-3 and PTP-1B was achieved in the whole brain and was not cell-type specific. Peptidic hormone and cytokine effects are not confined to the hypothalamus and leptin, for example, modulates the mesolimbic dopamine system (5,7,9) and long-term depression in the hippocampus (50). Hence, other behaviors than those reported here may be altered in the double mutants. In addition, the JAK/STAT pathway is involved in cell proliferation and SOCS-3 and PTP-1B suppress this pathway. Although we did not observe any gross histological abnormalities in brain of mutant mice, we cannot rule out that inactivation of *Socs-3* and *Ptpn1* may in turn affect

neural development as well as neurogenesis in adulthood (51).

We here provided evidence that abolishing both SOCS-3 and PTP-1B cytokine suppressor activities in brain is beneficial for body weight and glucose homeostasis because of their additive effects for most of the investigated phenotypes. We also found evidence for protein-specific roles and for synergism in the case of body length. Importantly, our study suggests that using a combination of inhibitors for SOCS-3 and PTP-1B may improve therapeutic trials targeting obesity and type 2 diabetes.

REFERENCES

1. Zhang Y, Proenca R, Maffei M, Barone M, Leopold L, Friedman JM. Positional cloning of the mouse obese gene and its human homologue. Nature 1994;372:425–432
2. Balthasar N, Coppari R, McMinn J, Liu SM, Lee CE, Tang V, Kenny CD, McGovern RA, Chua SC, Jr, Elmquist JK, Lowell BB. Leptin receptor signaling in POMC neurons is required for normal body weight homeostasis. Neuron 2004;42:983–991
3. Bingham NC, Anderson KK, Reuter AL, Stallings NR, Parker KL. Selective loss of leptin receptors in the ventromedial hypothalamic nucleus results in increased adiposity and a metabolic syndrome. Endocrinology 2008;149: 2138–2148
4. Dhillon H, Zigman JM, Ye C, Lee CE, McGovern RA, Tang V, Kenny CD, Christiansen LM, White RD, Edelstein EA, Coppari R, Balthasar N, Cowley MA, Chua S Jr, Elmquist JK, Lowell BB. Leptin directly activates SF1 neurons in the VMH, and this action by leptin is required for normal body-weight homeostasis. Neuron 2006;49:191–203
5. Fulton S, Pissios P, Manchon RP, Stiles L, Frank L, Pothos EN, Maratos-Flier E, Flier JS. Leptin regulation of the mesoaccumbens dopamine pathway. Neuron 2006;51:811–822
6. Grill HJ, Schwartz MW, Kaplan JM, Foxhall JS, Breininger J, Baskin DG. Evidence that the caudal brainstem is a target for the inhibitory effect of leptin on food intake. Endocrinology 2002;143:239–246
7. Hommel JD, Trinko R, Sears RM, Georgescu D, Liu ZW, Gao XB, Thurmon JJ, Marinelli M, DiLeone RJ. Leptin receptor signaling in midbrain dopamine neurons regulates feeding. Neuron 2006;51:801–810
8. Huo L, Maeng L, Bjorbaek C, Grill HJ. Leptin and the control of food intake: neurons in the nucleus of the solitary tract are activated by both gastric distension and leptin. Endocrinology 2007;148:2189–2197
9. Leinninger GM, Jo YH, Leshan RL, Louis GW, Yang H, Barrera JG, Wilson H, Opland DM, Faouzi MA, Gong Y, Jones JC, Rhodes CJ, Chua S Jr, Diano

S, Horvath TL, Seeley RJ, Becker JB, Munzberg H, Myers MG Jr. Leptin acts via leptin receptor-expressing lateral hypothalamic neurons to modulate the mesolimbic dopamine system and suppress feeding. Cell Metab 2009;10:89–98

10. Yadav VK, Oury F, Suda N, Liu ZW, Gao XB, Confavreux C, Klemenhagen KC, Tanaka KF, Gingrich JA, Guo XE, Tecott LH, Mann JJ, Hen R, Horvath TL, Karsenty G. A serotonin-dependent mechanism explains the leptin regulation of bone mass, appetite, and energy expenditure. Cell 2009;138: 976–989

11. Heymsfield SB, Greenberg AS, Fujioka K, Dixon RM, Kushner R, Hunt T, Lubina JA, Patane J, Self B, Hunt P, McCamish M. Recombinant leptin for weight loss in obese and lean adults: a randomized, controlled, dose-escalation trial. JAMA 1999;282:1568–1575

12. Hukshorn CJ, Saris WH, Westerterp-Plantenga MS, Farid AR, Smith FJ, Campfield LA. Weekly subcutaneous pegylated recombinant native human leptin (PEG-OB) administration in obese men. J Clin Endocrinol Metab 2000;85:4003–4009

13. Frederich RC, Hamann A, Anderson S, Lollmann B, Lowell BB, Flier JS. Leptin levels reflect body lipid content in mice: evidence for diet-induced resistance to leptin action. Nat Med 1995;1:1311–1314

14. Banks WA, Coon AB, Robinson SM, Moinuddin A, Shultz JM, Nakaoke R, Morley JE. Triglycerides induce leptin resistance at the blood-brain barrier. Diabetes 2004;53:1253–1260

15. Caro JF, Kolaczynski JW, Nyce MR, Ohannesian JP, Opentanova I, Goldman WH, Lynn RB, Zhang PL, Sinha MK, Considine RV. Decreased cerebrospinal-fluid/serum leptin ratio in obesity: a possible mechanism for leptin resistance. Lancet 1996;348:159–161

16. El-Haschimi K, Pierroz DD, Hileman SM, Bjorbaek C, Flier JS. Two defects contribute to hypothalamic leptin resistance in mice with diet-induced obesity. J Clin Invest 2000;105:1827–1832

17. Schwartz MW, Peskind E, Raskind M, Boyko EJ, Porte D Jr. Cerebrospinal fluid leptin levels: relationship to plasma levels and to adiposity in humans. Nat Med 1996;2:589–593

18. Ozcan L, Ergin AS, Lu A, Chung J, Sarkar S, Nie D, Myers MG Jr, Ozcan U. Endoplasmic reticulum stress plays a central role in development of leptin resistance. Cell Metab 2009;9:35–51

19. Zhang K, Kaufman RJ. From endoplasmic-reticulum stress to the inflammatory response. Nature 2008;454:455–462

20. Howard JK, Flier JS. Attenuation of leptin and insulin signaling by SOCS proteins. Trends Endocrinol Metab. 2006;17:365–371;Epub 2006 Sep 2028

21. Munzberg H, Myers MG Jr. Molecular and anatomical determinants of central leptin resistance. Nat Neurosci 2005;8:566–570

22. Goldstein BJ, Ahmad F, Ding W, Li PM, Zhang WR. Regulation of the insulin signalling pathway by cellular protein-tyrosine phosphatases. Mol Cell Biochem 1998;182:91–99

23. Zabolotny JM, Bence-Hanulec KK, Stricker-Krongrad A, Haj F, Wang Y, Minokoshi Y, Kim YB, Elmquist JK, Tartaglia LA, Kahn BB, Neel BG. PTP1B regulates leptin signal transduction in vivo. Dev Cell 2002;2:489–495

24. Buettner C, Pocai A, Muse ED, Etgen AM, Myers MG Jr, Rossetti L. Critical role of STAT3 in leptin's metabolic actions. Cell Metab 2006;4:49–60

25. Bjorbaek C, Elmquist JK, Frantz JD, Shoelson SE, Flier JS. Identification of SOCS-3 as a potential mediator of central leptin resistance. Mol Cell 1998;1:619–625

26. Bjorbaek C, El-Haschimi K, Frantz JD, Flier JS. The role of SOCS-3 in leptin signaling and leptin resistance. J Biol Chem 1999;274:30059–30065

27. Elias CF, Aschkenasi C, Lee C, Kelly J, Ahima RS, Bjorbaek C, Flier JS, Saper CB, Elmquist JK. Leptin differentially regulates NPY and POMC neurons projecting to the lateral hypothalamic area. Neuron 1999;23:775–786

28. Munzberg H, Flier JS, Bjorbaek C. Region-specific leptin resistance within the hypothalamus of diet-induced obese mice. Endocrinology 2004;145: 4880–4889

29. Lam NT, Lewis JT, Cheung AT, Luk CT, Tse J, Wang J, Bryer-Ash M, Kolls JK, Kieffer TJ. Leptin increases hepatic insulin sensitivity and protein tyrosine phosphatase 1B expression. Mol Endocrinol 2004;18:1333–1345

30. Morrison CD, White CL, Wang Z, Lee SY, Lawrence DS, Cefalu WT, Zhang ZY, Gettys TW. Increased hypothalamic protein tyrosine phosphatase 1B contributes to leptin resistance with age. Endocrinology 2007;148:433–440

31. White CL, Whittington A, Barnes MJ, Wang Z, Bray GA, Morrison CD. HF diets increase hypothalamic PTP1B and induce leptin resistance through

both leptin-dependent and -independent mechanisms. Am J Physiol Endocrinol Metab 2009;296:E291–E299

32. Zabolotny JM, Kim YB, Welsh LA, Kershaw EE, Neel BG, Kahn BB. Protein-tyrosine phosphatase 1B expression is induced by inflammation in vivo. J Biol Chem 2008;283:14230–14241

33. Howard JK, Cave BJ, Oksanen LJ, Tzameli I, Bjorbaek C, Flier JS. Enhanced leptin sensitivity and attenuation of diet-induced obesity in mice with haploinsufficiency of Socs3. Nat Med 2004;10:734–738

34. Mori H, Hanada R, Hanada T, Aki D, Mashima R, Nishinakamura H, Torisu T, Chien KR, Yasukawa H, Yoshimura A. Socs3 deficiency in the brain elevates leptin sensitivity and confers resistance to diet-induced obesity. Nat Med 2004;10:739–743

35. Bence KK, Delibegovic M, Xue B, Gorgun CZ, Hotamisligil GS, Neel BG, Kahn BB. Neuronal PTP1B regulates body weight, adiposity and leptin action. Nat Med 2006;12:917–924

36. Elchebly M, Payette P, Michaliszyn E, Cromlish W, Collins S, Loy AL, Normandin D, Cheng A, Himms-Hagen J, Chan CC, Ramachandran C, Gresser MJ, Tremblay ML, Kennedy BP. Increased insulin sensitivity and obesity resistance in mice lacking the protein tyrosine phosphatase-1B gene. Science 1999;283:1544–1548

37. Klaman LD, Boss O, Peroni OD, Kim JK, Martino JL, Zabolotny JM, Moghal N, Lubkin M, Kim YB, Sharpe AH, Stricker-Krongrad A, Shulman GI, Neel BG, Kahn BB. Increased energy expenditure, decreased adiposity, and tissue-specific insulin sensitivity in protein-tyrosine phosphatase 1B-deficient mice. Mol Cell Biol 2000;20:5479–5489

38. Yasukawa H, Ohishi M, Mori H, Murakami M, Chinen T, Aki D, Hanada T, Takeda K, Akira S, Hoshijima M, Hirano T, Chien KR, Yoshimura A. IL-6 induces an anti-inflammatory response in the absence of SOCS3 in macrophages. Nat Immunol 2003;4:551–556

39. Zhang R, Dhillon H, Yin H, Yoshimura A, Lowell BB, Maratos-Flier E, Flier JS. Selective inactivation of Socs3 in SF1 neurons improves glucose homeostasis without affecting body weight. Endocrinology 2008;149:5654–5661

40. Koren S, Fantus IG. Inhibition of the protein tyrosine phosphatase PTP1B: potential therapy for obesity, insulin resistance and type-2 diabetes mellitus. Best Pract Res Clin Endocrinol Metab 2007;21:621–640

41. Lee S, Wang Q. Recent development of small molecular specific inhibitor of protein tyrosine phosphatase 1B. Med Res Rev 2007;27:553–573

42. Kokkotou E, Jeon JY, Wang X, Marino FE, Carlson M, Trombly DJ, Maratos-Flier E. Mice with MCH ablation resist diet-induced obesity through strain-specific mechanisms. Am J Physiol Regul Integr Comp Physiol. 2005;289:R117–R124

43. Forni PE, Scuoppo C, Imayoshi I, Taulli R, Dastru W, Sala V, Betz UA, Muzzi P, Martinuzzi D, Vercelli AE, Kageyama R, Ponzetto C. High levels of Cre expression in neuronal progenitors cause defects in brain development leading to microencephaly and hydrocephaly. J Neurosci 2006;26: 9593–9602

44. Gu F, Dube N, Kim JW, Cheng A, Ibarra-Sanchez Mde J, Tremblay ML, Boisclair YR. Protein tyrosine phosphatase 1B attenuates growth hormone-mediated JAK2-STAT signaling. Mol Cell Biol 2003;23:3753–3762

45. Buckley DA, Cheng A, Kiely PA, Tremblay ML, O'Connor R. Regulation of insulin-like growth factor type I (IGF-I) receptor kinase activity by protein tyrosine phosphatase 1B (PTP-1B) and enhanced IGF-I-mediated suppression of apoptosis and motility in PTP-1B-deficient fibroblasts. Mol Cell Biol 2002;22:1998–2010

46. Greenhalgh CJ, Alexander WS. Suppressors of cytokine signalling and regulation of growth hormone action. Growth Horm IGF Res 2004;14:200–206

47. Yadav A, Kalita A, Dhillon S, Banerjee K. JAK/STAT3 pathway is involved in survival of neurons in response to insulin-like growth factor and negatively regulated by suppressor of cytokine signaling-3. J Biol Chem 2005;280:31830–31840

48. Hinoi E, Gao N, Jung DY, Yadav V, Yoshizawa T, Myers MG, Jr, Chua SC, Jr, Kim JK, Kaestner KH, Karsenty G. The sympathetic tone mediates leptin's inhibition of insulin secretion by modulating osteocalcin bioactivity. J Cell Biol 2008;183:1235–1242

49. Tran TT, Yamamoto Y, Gesta S, Kahn CR. Beneficial effects of subcutaneous fat transplantation on metabolism. Cell Metab 2008;7:410–420

50. Moult PR, Milojkovic B, Harvey J. Leptin reverses long-term potentiation at hippocampal CA1 synapses. J Neurochem 2009;108:685–696

51. Kokoeva MV, Yin H, Flier JS. Neurogenesis in the hypothalamus of adult mice: potential role in energy balance. Science 2005;310:679–683